Computers and Concrete, *Vol. 17, No. 4 (2016) 553-566*
DOI: http://dx.doi.org/10.12989/cac.2016.17.4.553

Effect of basalt fibers on fracture energy and mechanical properties of HSC

Mehmet E. Arslan*

Department of Civil Engineering, Technology Faculty Düzce University, 81620, Turkey

(Received February 8, 2016, Revised February 19, 2016, Accepted March 1, 2016)

Abstract. Fracture energy is one of the key parameters reveal cracking resistance and fracture toughness of concrete. The main purpose of this study is to determine fracture behavior, mechanical properties and microstructural analysis of high strength basalt fiber reinforced concrete (HSFRC). For this purpose, three-point bending tests were performed on notched beams produced using HSFRCs with 12 mm and 24mm fiber length and 1, 2 and 3 kg/m³ fiber content in order to determine the value of fracture energy. Fracture energies of the notched beam specimens were calculated by analyzing load versus crack mouth opining displacement curves by the help of RILEM proposal. The results show that the effects of basalt fiber content and fiber length on fracture energy are very significant. The splitting tensile and flexural strength of HSFRC increased with increasing fiber content whereas a slight drop in flexural strength was observed for the mixture with 24mm fiber length and 3 kg/m³ fiber content. On the other hand, there was no significant effect of fiber addition on the compressive strength and modulus of elasticity of the mixtures. In addition, microstructural analysis of the three components; cement paste, aggregate and basalt fiber were performed based on the Scanning Electron Microscopy and Energy-Dispersive X-ray Spectroscopy examinations.

Keywords: basalt fiber; high strength concrete; mechanical properties; fracture energy; microstructure

1. Introduction

Fibers have been used for a long time in numerous fields of study. Recently, new fibers have been utilized in cement and concrete materials parallel to the development in technology and textile industry. The most popular fibers used in composites are glass, carbon, aramid, polypropylene, and basalt. Due to their limited dimensions, fibers show an outstanding structural perfection. This feature conveys, high breaking stress, very high tensile modulus, linear elastic behavior up to failure (Kabay 2014, Sümer and Aktaş 2014, Kizilkanat *et al.* 2015). Fibers are used generally to improve flexural strength, toughness, load carrying, impact, fatigue and abrasion resistance, deformation capability capacity after cracking, ductility and plastic cracking characteristics of concrete. In addition fibers help controlling of cracks and they affect failure modes of concrete members (Sümer and Aktaş 2011, Murthy *et al.* 2013, Shaikh 2013, Aktas and Sumer 2014, Brigante 2014, Jiang *et al.* 2014, Li *et al.* 2014, Tassew and Lubell 2014, Fiore *et al.*

*Corresponding author, Assistant Professor, E-mail: mehmeteminarslan@duzce.edu.tr

http://www.techno-press.org/?journal=cac&subpage=8 ISSN: 1598-8198 (Print), 1598-818X (Online)

2015, Lee *et al.* 2015, Pehlivanlı *et al.* 2015).

Basalt is a volcanic igneous rock which performs well in terms of strength, temperature range, and durability (Di Ludovico *et al.* 2010, Kabay 2014). Basalt fibers (BF) are obtained from basalt rocks after melting process. BFs usually have a diameter ranging from 13 to 20μm. BFs are excellent thermal and acoustic insulators, and they preserve their mechanical properties even at high temperature. Resulting from the melting of a single raw material, BFs have higher performance than other fibers in terms of heat protection, thermal and acoustic insulation, durability, and vibration resistance (Brigante 2014). Also they are quite cheap, despite their features, which are significantly better than other similar materials employed today, such as glass fiber. It is known that the BFs have better tensile strength than the E-glass fibers, greater failure strain than the carbon fibers as well as good resistance to chemical attack, impact load and fire with less poisonous fumes (Sim *et al.* 2005, Kabay 2014). Even if BF has aforementioned advantages, studies about BF are limited (Dias and Thaumaturgo 2005, Li and Xu 2009, Jiang *et al.* 2014). Therefore further experimental studies should be conducted on determining the effects of BF on physical and mechanical properties of composites.

Fracture energy of concrete is one of the most important parameter for understanding the properties of concrete. The most widely used fracture mechanics model for analyzing concrete structures is the fictitious crack model (FCM) proposed by Hillerborg (Hillerborg 1983, Hillerborg 1985). Fracture energy (G_f) is the energy needed to develop one crack completely. RILEM (FMC-50 1985) and Peterson (1980) recommended a method for the determination of G_f using simple three-point bending test.

One of the major roles of fiber in concrete is to increase the fracture energy (Bayramov *et al.* 2004, Şahin and Köksal 2011). Although several types of fibers have been used in concrete, knowledge related to mechanical properties, fracture behavior and microstructure of high strength concrete with BF is insufficient. The main purpose of this study is to determine mechanical properties, fracture behaviors and to investigate microstructure of high strength basalt fiber reinforced concrete (HSFRC). For such purposes, three-point bending tests were performed on notched beams produced using HSFRCs with two fiber length (12 mm and 14 mm) and three fiber BF contents (1, 2 and 3 kg/m^3) in order to determine the value of fracture energy.

2. Experimental study

2.1 Materials and test specimens

Table 1 Mixture proportion of the concrete

Concrete Code	Fiber Content (kg/m^3)	Cement (kg/m^3)	W/C Ratio	Coarse Aggregate (5-12 mm) (kg/m^3)	Fine Aggregate (0-5 mm) (kg/m^3)	Super plasticizer (kg/m^3)
Ref	-					
HSFRC-12-1	1					
HSFRC-12-2	2					
HSFRC-12-3	3	500	0.35	688	1032	7.5
HSFRC-24-1	1					
HSFRC-24-2	2					
HSFRC-24-3	3					

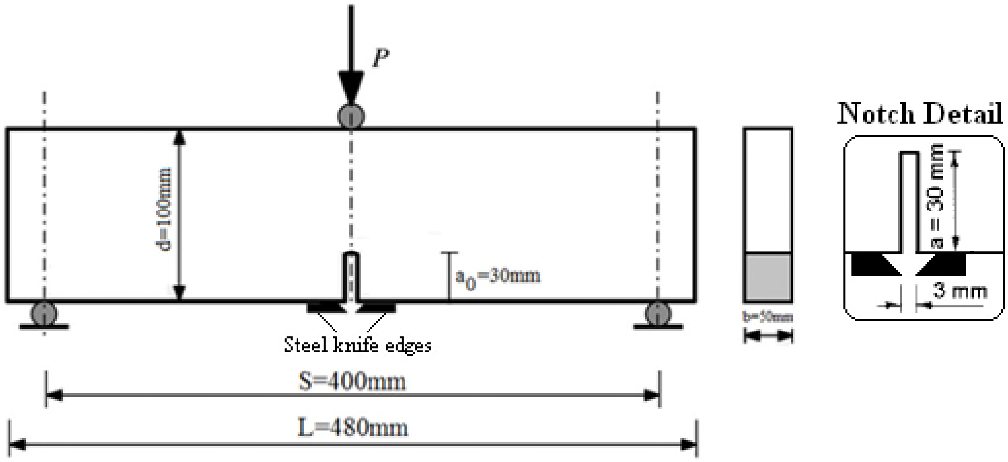

Fig. 1 Dimensions and details of notched beam test specimens

Table 2 Properties of basalt fiber

Fiber Length (mm)	Diameter (μm)	Modulus of Elasticity (GPa)	Elongation (%)	Tensile Strength (MPa)	Density (g/cm^3)
12-24	13-20	88	3.15	4000-4500	2.80

Fig. 2 12 mm and 24mm basalt fibers

In the current study, CEM I 42.5R Portland cement was used for producing of HSFRCs and Reference (Ref) specimens. The mixture proportions of Ref and HSFRCs are given in Table 1. The water/cement ratio is kept constant as 0.35 for all mixtures. In this study, fine (0-5 mm) and course (5-12 mm) limestone aggregates were used. The amount of high-range water reducing admixture was kept constant as 1.5% by weight of cement used in concrete mixtures to maintain sufficient workability.

In order to determine the fracture properties of Ref and HSFRCs, 21 notched beams were tested by three point bending test. The dimensions of all specimens were 50 mm×100 mm×480 mm with a notch height to beam height ratio (a_0/d) equal to 0.3 and a free span to beam height ratio (S/d)

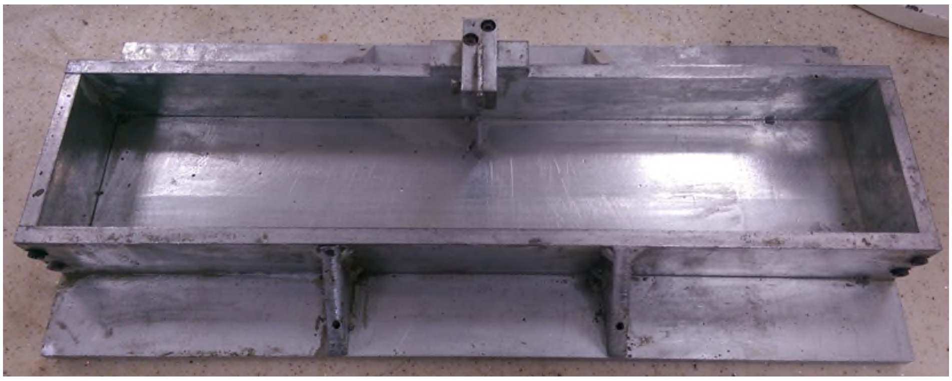

Fig. 3 Steel mold used to produce notched beam test specimens

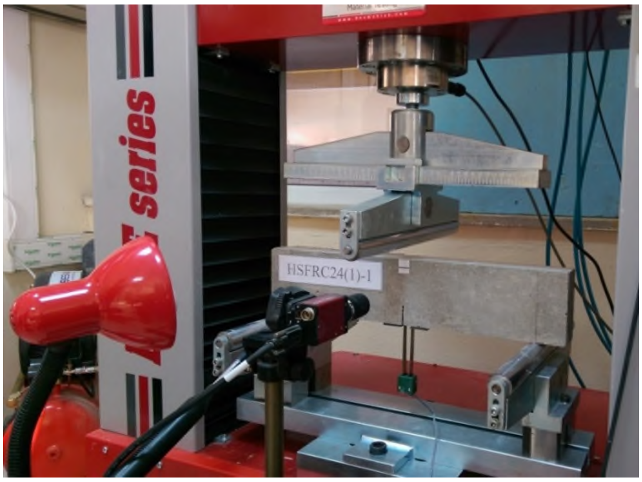

Fig. 4 Three-point bending test set-up

equal to 4. Details of the notched beam specimen are given in Fig. 1.

Two types of fiber length (12 mm and 24 mm) and three different BF content (1, 2 and 3 kg/m³) were used to reveal the effects of BF on mechanical and fractural behavior of HSFRCs. Detailed properties provided by manufacturer and BFs are presented in Table 2 and Fig. 2 (Kabay 2014, Kizilkanat *et al.* 2015). Modular steel molds having a plate constructed inside to form notches have been used to produce the notched beam specimens (Fig. 3).

2.2 Method

Compressive strength tests have been carried out on three 150×300 mm cylinders specimens and averages of the test results were obtained for each series. Splitting tensile strengths of 150 mm cube specimens were calculated using the following expression

$$f_{st} = 2P/\pi a^2 \tag{1}$$

where P, and a are the ultimate load and edge dimensions of the specimen, respectively.

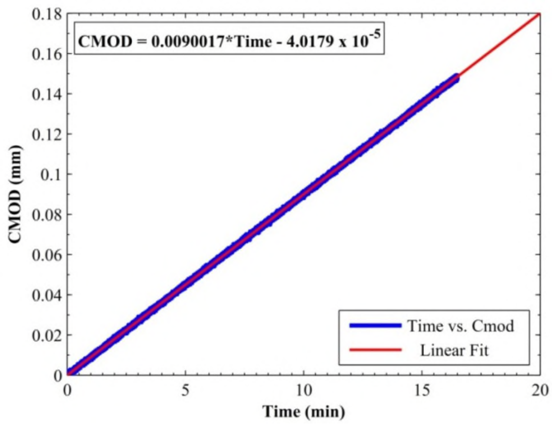

Fig. 5 Time-CMOD relation of three-point bending test

Displacement controlled loading achieved by using Universal Test Machine (Fig. 4). Time versus Crack Mouth Opening Displacement (CMOD) relation is recorded as in Fig. 5. This relation is almost linear. Loading speed of the three-point bending test was determined as 0.009 mm/min (Fig. 5). End of test were determined as 95% drop in peak load for all the specimens.

CMOD was measured by using a clip gauge installed at the center of the notch with the help of steel knife edges. A video-extensometer was used to measure the deflection at the mid-span. Fracture energy (G_f) was calculated by the help of the RILEM (FMC-50 1985) proposal given in Eq. (2).

$$G_f = \frac{W_0 + mg\delta}{A} \tag{2}$$

where W_0 is the area under the load-CMOD curve (N/m), mg is the self-weight of the specimen between supports (kg), δ is the maximum displacement (m), and A is the fracture area [b(d-a_0)] (m^2); b and d are the width and height of the beam, respectively. Flexural strength of concretes was calculated using three-point bending test results with following expression:

$$f = \frac{3PS}{2b\left(d - a_0\right)^2} \tag{3}$$

where P is the maximum load, S is the span length, b is width of specimen, d is height of specimen, and a_0 is notch depth. Modulus of elasticity (E) of the HSFRC is calculated from the measured initial compliance C_i of load-CMOD curve using Eq.(4). (Bažant 1992, Shah 1995)

$$E = \frac{6Sa_0V_1(\alpha)}{\left(C_i bd^2\right)} \tag{4}$$

where $V_1(\alpha)$ is a function (Eq. (5)) dependent on (α=(a_0+h_0)/(d+h_0)) and h_0 thickness of steel knife edge,

$$V_1(\alpha) = 0.76 - 2.38\alpha + 3.87\alpha^2 - 2.04\alpha^3 + 0.66\big/(1-\alpha)^2 \tag{5}$$

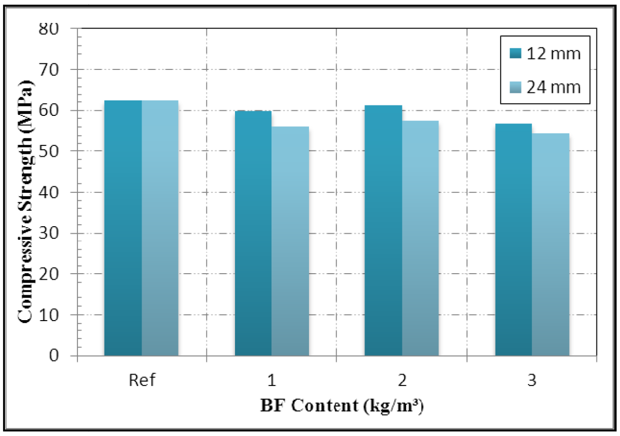

Fig. 6 Compressive strengths of the mixtures

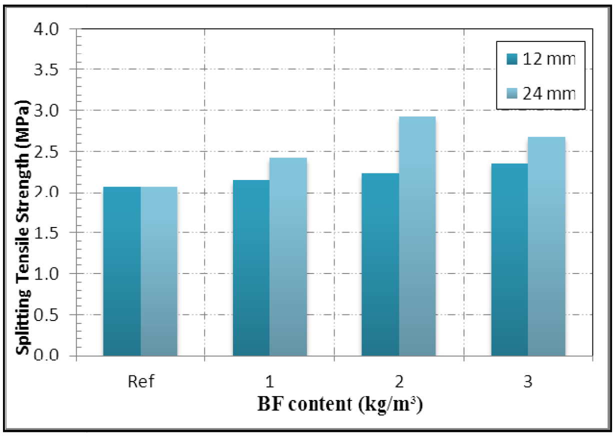

Fig. 7 Splitting tensile strengths of the mixtures

3. Results and discussions

3.1 Compressive strength

Average compressive strength of Ref and HSFRCs obtained from cylinder specimens are given in Fig. 6. There is no significant effect of different fiber lengths (12 mm and 24 mm) and fiber contents (1, 2 and 3 kg/m³) on compressive strength. Thus, the effect of length and content of BF on compressive strength is not consistent. Maximum decrease approximately by 12% is occurred in HSFRC-24-3 when compared to Ref specimen. On the other hand, the addition of BF into concrete may have an effect on increasing the ductility in the compressive failure rather than the compressive strength.

3.2 Splitting tensile and flexural strength

Splitting tensile strength results of mixtures are given in Fig. 7. Patel *et al.* (2012) and

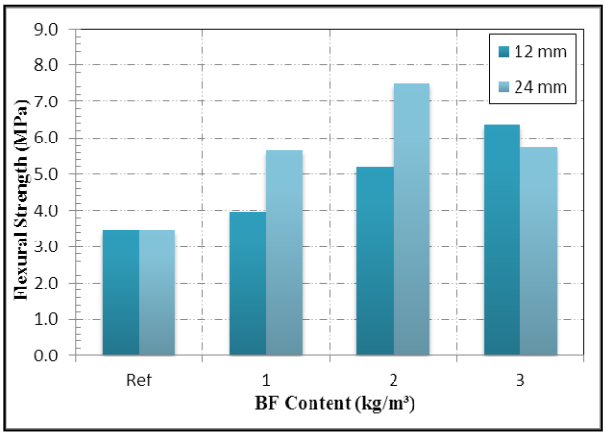

Fig. 8 Flexural strengths of the mixtures

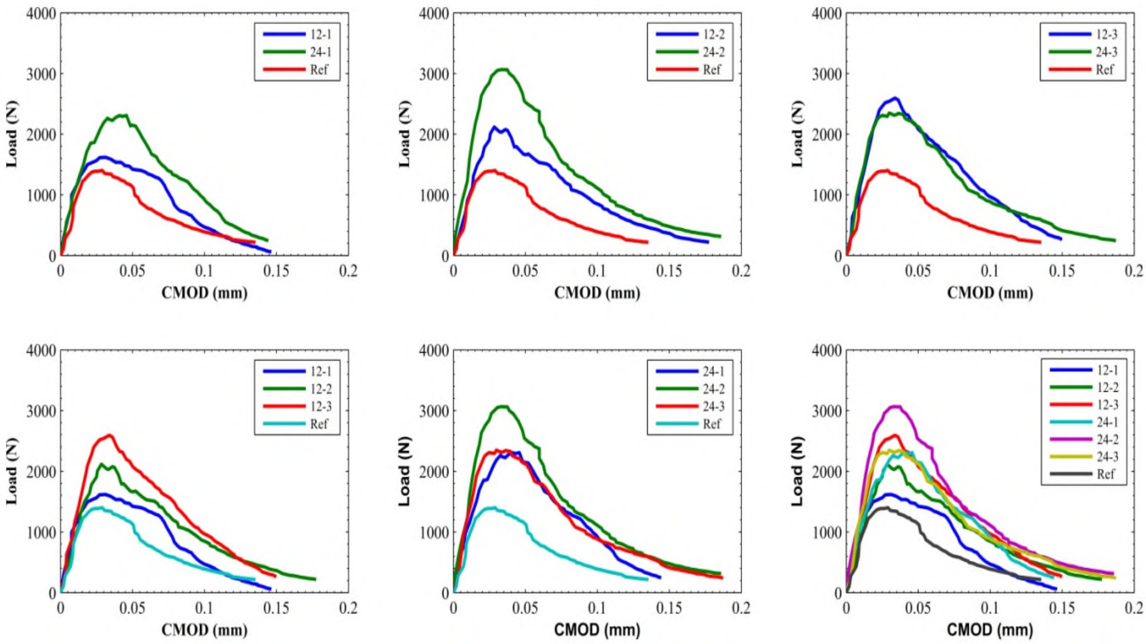

Fig. 9 Load-CMOD responses of three-point bending tests

Kizilkanat *et al.* (2015) reported that splitting tensile test is not an accurate estimation of direct tensile strength due to mixed stress field and different fiber orientation. They also have expressed that it gives idea about the ductility of the material. In this study, it was obtained from the test, HSRFC specimens did not separate out after first cracking unlike Ref specimen. This result shows that BFs enhance ductility of Ref specimen which originally exhibited brittle behavior. In addition BFs increased the splitting tensile strength of HSFRCs. Maximum increase (29%) occurred in HSFRC-24-2 compared to Ref specimen. However, the increase in splitting tensile strength began to decrease for HSFRC-24-3 specimen.

Flexural strength values of Ref and HSFRC specimens obtained from three-point bending test

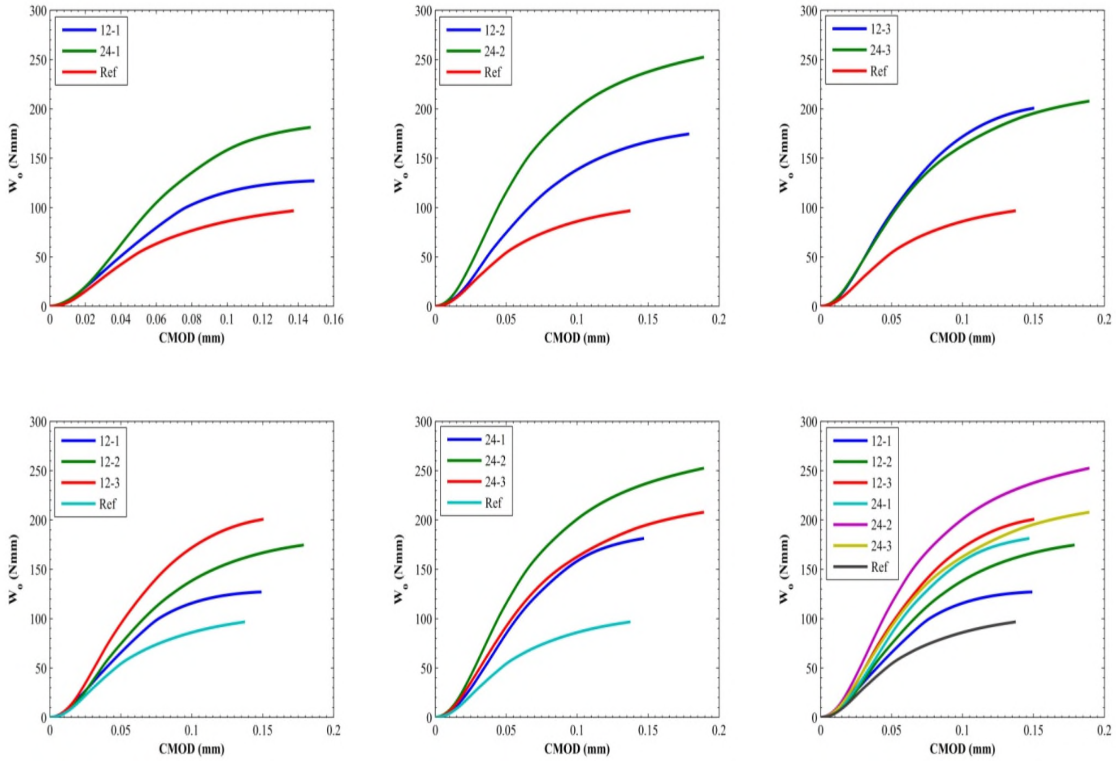

Fig. 10 Changing of W_0 corresponding to CMOD

are given in Fig. 8. BF addition considerably increased flexural strengths of HSFRCs with respect to Ref specimen. Increase in flexural strengths is more apparent for the concrete mixtures in which 24 mm BF with different content has been used. While for all contents of 12 mm BF increased constantly flexural strength of HSFRCs, for 24 mm BF with 3 kg/m³ fiber content a slight drop in flexural strength was observed in flexural strength in comparison to 2 kg/m³ BF content. Highest flexural strength occurred in HSFRC-24-2 (7.51MPa) mixture.

3.3 Fracture energy and modulus of elasticity

Load-CMOD curves of three-point bending test of notched beam specimens are given in Fig. 9. Load-CMOD curve of test specimens having the same fiber content with different fiber length and having the same fiber length with different fiber content were drown separately to demonstrate effects of fiber length and fiber content more clearly. In addition all the load-CMOD curves were given collectively to make relative comparison between fiber lengths and fiber contents. It is apparent from Fig. 9 that HSFRC-24-2 has the highest load carrying capacity. Although for all the contents of 12 mm BF reached peak loads were increased, for HSFRC-24-3 test specimen peak load decreased. However, the observed peak load was still higher than Ref and the test specimens with all the content of 12 mm BF.

G_f of Ref and HSFRC notched beam specimens with different fiber length and content were determined using area under the load-CMOD curves (W_0) according to Eq. (2). Changing of W_0

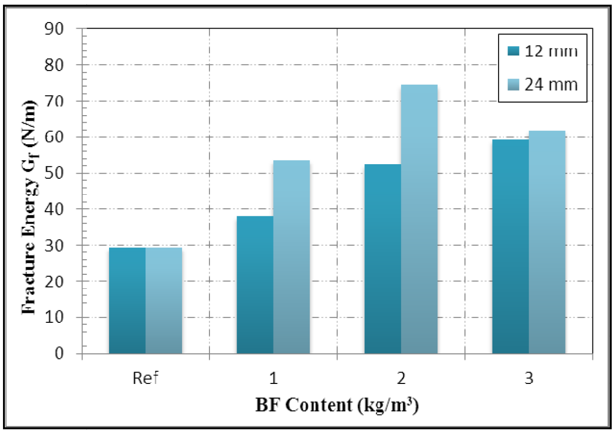

Fig. 11 Fracture Energies of notched beam specimens

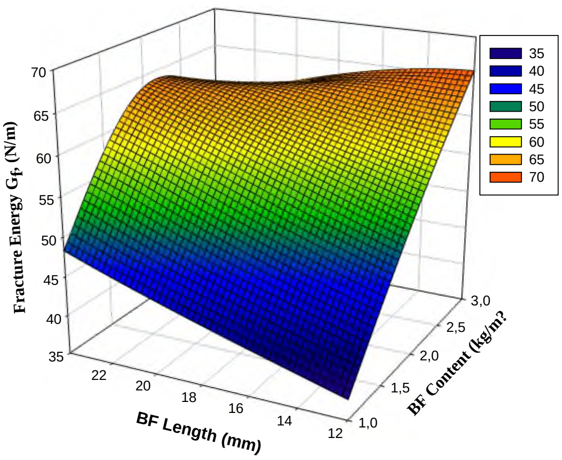

Fig. 12 Variation of Fracture Energy with fiber length and content

corresponding to CMOD and calculated G_f values of the test specimens are illustrated in Fig. 10 and Fig. 11, respectively.

It can be seen from Fig. 11 that BF addition considerable increases the G_f values of test specimens compared to that of Ref test specimen. As it was expected, a slight drop in fracture energy was observed in HSFRC-24-3. In addition, effects of fiber length can be distinguished more clearly that 24 mm BF increased G_f of the notched beam specimens more than those of 12 mm BF. The highest G_f was obtained for HSFRC-24-2 (74.64 N/m) test specimen that is 2.5 times of Ref test specimen. It is thought that the reason for the increase in G_f with increasing fiber content stems from a great number of BFs forming tortuous connection in the crack propagation. Variation of fracture energy with BF length and BF content are given in Fig. 12. As seen from the figure a peak G_f value was obtained for the fiber contents of 24mm BF whereas G_f values of the fiber contents of 12 mm still have tendency of increasing.

Modulus of elasticity values of the notched beam specimens were determined by the help of Eq. (4) using the results of three-point bending test and results are given in Fig. 13. Also the modulus of elasticity values were compared with the values calculated using Eq. (6) proposed by

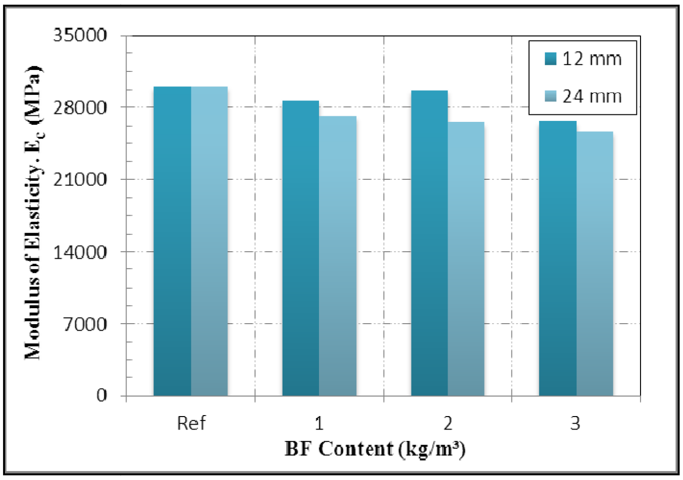

Fig. 13 Modulus of elasticity values calculated using three-point bending test results

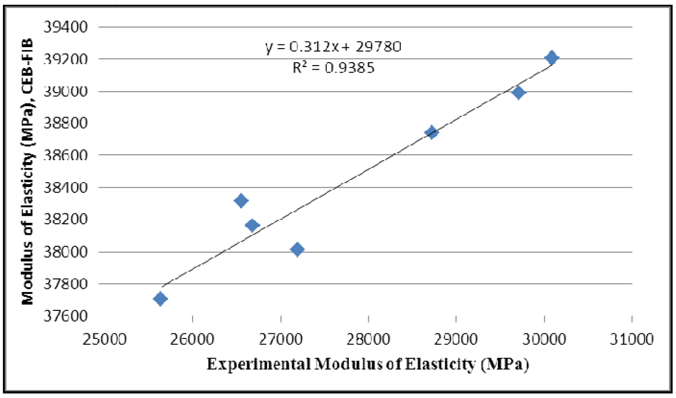

Fig. 14 Relation between experimental and calculated modulus of elasticity

Table 3 Mechanical properties and fracture energy values of Ref and HSFRC specimens

Concrete Code	Compressive Strength (MPa)	Splitting Tensile Strength (MPa)	Flexural Strength (MPa)	Fracture Energy (N/m)	Modulus of Elasticity (MPa)
Ref	62.30	2.07	3.45	29.48	30091
HSFRC-12-1	59.80	2.15	3.96	38.25	28728
HSFRC-12-2	61.13	2.23	5.18	52.28	29714
HSFRC-12-3	56.83	2.36	6.35	59.38	26683
HSFRC-24-1	56.06	2.42	5.65	53.74	27197
HSFRC-24-2	57.60	2.93	7.51	74.64	26558
HSFRC-24-3	54.53	2.68	5.75	61.92	25640

CEB-FIB (1990) and regression analysis was made to establish a function (Fig. 14). Although modulus of elasticity values calculated using CEB-FIB (1990) are higher than those observed from experiments, high correlation coefficient was obtained. On the other hand, the modulus of elasticity of fiber reinforced concretes slightly reduced with fiber content compared to Ref test

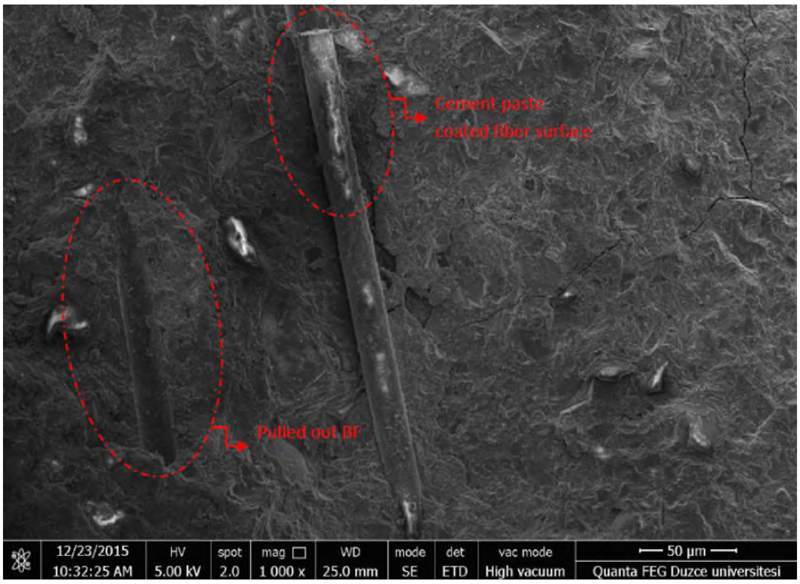

Fig. 15 SEM image (1000x) of the HSFRC-24-2 test specimen

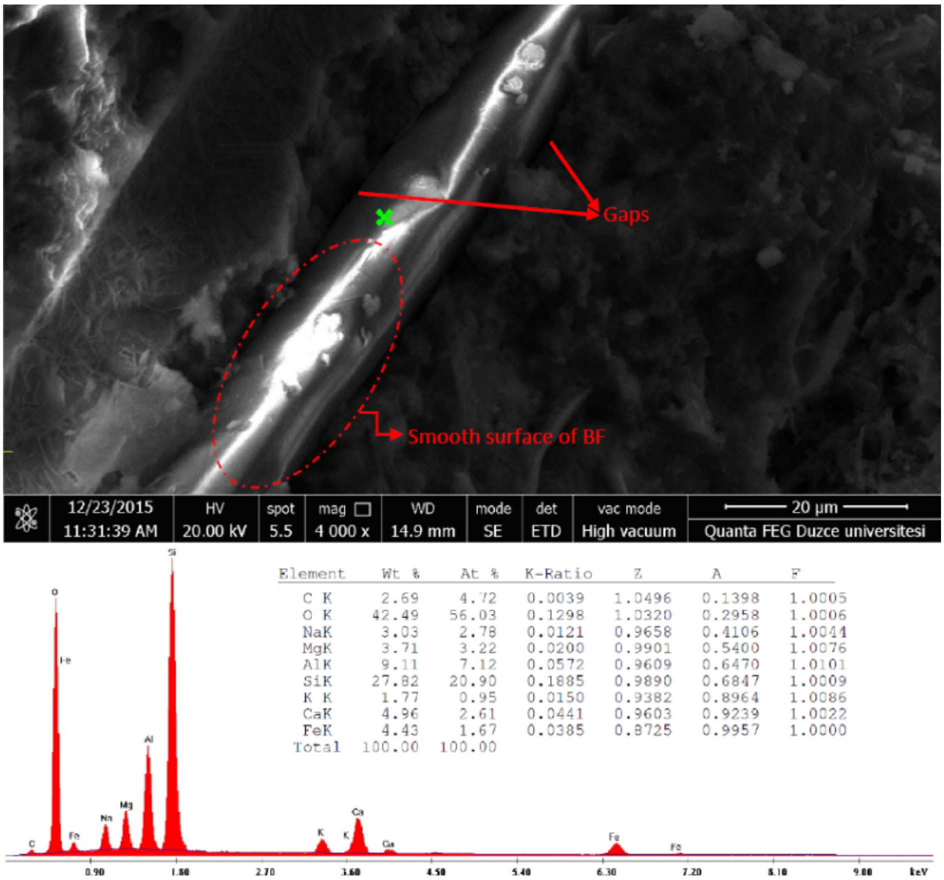

Element	Wt %	At %	K-Ratio	Z	A	F
C K	2.69	4.72	0.0039	1.0496	0.1398	1.0005
O K	42.49	56.03	0.1298	1.0320	0.2958	1.0006
NaK	3.03	2.78	0.0121	0.9658	0.4106	1.0044
MgK	3.71	3.22	0.0200	0.9901	0.5400	1.0076
AlK	9.11	7.12	0.0572	0.9609	0.6470	1.0101
SiK	27.82	20.90	0.1885	0.9890	0.6847	1.0009
K K	1.77	0.95	0.0150	0.9382	0.8964	1.0086
CaK	4.96	2.61	0.0441	0.9603	0.9239	1.0022
FeK	4.43	1.67	0.0385	0.8725	0.9957	1.0000
Total	100.00	100.00				

Fig. 16 SEM and EDX analysis of HSFRC

specimen. Modulus of elasticity values are between 30091-25640 MPa and maximum decrease in the modulus of elasticity occurred by 15% for HSFRC-24-3 mixture.

$$E = 9500\left(\sigma + 8\right)^{1/3} \tag{6}$$

Mechanical properties and fracture energy values obtained from cube, cylinder and notched beam specimens are given in Table 3.

3.4 Microstructural analysis

Microstructural analysis of the three components; cement paste, aggregate and basalt fiber were performed based on the Scanning Electron Microscopy (SEM) and Energy-Dispersive X-ray Spectroscopy (EDX) examinations. Fig. 15 shows the SEM image (1000x) of the HSFRC-24-2 test specimen.

It is clearly seen from Fig. 15, specimen has Type III – a denser, almost spherical form of CSH gel morphologies. In addition, BFs have been partly coated with cement paste although it has smooth surfaces. Even if it is not possible to mention about perfect bonding because of the slippage of BF from cement paste, cement paste coated BF surfaces indicate existence of bond between cement paste and BF. Increases in flexural and splitting tensile strength also indicate contribution of BF on bond strength. On the other hand, none of BFs ruptured, due to its high tensile strength.

EDX results given in Fig. 16 show the composition of the BF is predominantly Si, from the large Si peaks. Composition also contains Al, Ca and Mg. Moreover, some gaps at interfacial transition zone stemming from the imperfect bond between BF and cement paste were observed.

4. Conclusions

In this study, mechanical properties, fracture behaviors and microstructure of HSFRC mixtures were determined. For these purposes, three-point bending tests were performed on notched beams produced using HSFRCs with two fiber length and 1, 2 and 3 kg/m³ BF contents in order to determine the value of fracture energy. Based on the results of this investigation, the following conclusions can be made:

• There is no significant and consistent effect of different BF lengths and contents on compressive strength. Maximum decrease approximately occurred by 12% in HSFRC-24-3 compared to Ref specimen.

• BFs increased the splitting tensile strength of HSFRCs. Maximum increase (29%) occurred in HSFRC-24-2 compared to Ref specimen. However, the increase in splitting tensile strength began to decrease for HSFRC-24-3 specimen.

• BF addition considerably increased flexural strengths of HSFRCs with respect to Ref specimen. Increase in flexural strengths is more apparent for HSFRC mixtures with 24 mm fiber length. Highest flexural strength occurred in HSFRC-24-2 mixture. While for all contents of 12 mm BF increased constantly flexural strength of HSFRCs, for HSFRC-24-3 specimen a slight drop in flexural strength was observed in flexural strength in comparison to HSFRC-24-2 specimen.

• BF addition considerable increases the G_f of test specimens compared to Ref specimen. The highest was obtained for HSFRC-24-2 test specimen that is 2.5 times of Ref specimen. It is thought that the reason for the increase in fracture energy with increasing fiber content stems from a great number of BFs forming tortuous connection in the crack propagation.

• The modulus of elasticity of fiber reinforced concretes slightly reduced with fiber content compared to Ref specimen. Modulus of elasticity values are between 30091-25640 MPa and maximum decrease in modulus of elasticity occurred as 15% for HSFRC-24-3 mixture.

• SEM image of HSFRC-24-2 specimen has showed that the specimen has Type III – a denser, almost spherical form of CSH gel morphologies. In addition, BFs have been partly coated with cement paste although it has smooth surfaces. Even if it is not possible to mention about perfect bonding because of the slippage of BF from cement paste, cement paste coated BF surfaces indicate existence of bond between cement paste and BF. Increases in flexural and splitting tensile strength also indicate contribution of BF on bond strength. On the other hand, none of BFs ruptured, since its high tensile strength.

References

Aktas, M. and Sumer, Y. (2014), "Nonlinear finite element analysis of damaged and strengthened reinforced concrete beams", *J. Civil Eng. Manage.*, **20**(2), 201-210.

Bayramov, F., Taşdemir, C. and Taşdemir, M.A. (2004), "Optimisation of steel fibre reinforced concretes by means of statistical response surface method", *Cement Concrete Compos.*, **26**(6), 665-675.

Bažant, Z.P. (1992), *Fracture Mechanics of Concrete Structures*, Taylor and Francis, New York, USA.

Brigante, D. (2014), *New Composite Materials: Selection, Design, and Application*, Springer International Publishing, Switzerland.

CEB-FIB (1990), CEB-FIP Model Code for Concrete Structures.

Di Ludovico, M., Prota, A. and Manfredi, G. (2010), "Structural upgrade using basalt fibers for concrete confinement", *J. Compos. Constr.*, **14**(5), 541-552.

Dias, D.P. and Thaumaturgo, C. (2005), "Fracture toughness of geopolymeric concretes reinforced with basalt fibers", *Cement Concrete Compos.*, **27**(1), 49-54.

Fiore, V., Scalici, T., Di Bella, G. and Valenza, A. (2015), "A review on basalt fibre and its composites", *Compos. Part B: Eng.*, **74**, 74-94.

FMC-50, R. (1985), "Determination of the fracture energy of mortar and concrete by means of three-point bend tests on notched beams", *Mater. Struct.*, **18**(4), 287-290.

Hillerborg, A. (1983), *Analysis of one single crack*, Elsevier.

Hillerborg, A. (1985), "The theoretical basis of a method to determine the fracture energy GF of concrete", *Mater. Struct.*, **18**(4), 291-296.

Jiang, C., Fan, K., Wu, F. and Chen, D. (2014), "Experimental study on the mechanical properties and microstructure of chopped basalt fibre reinforced concrete", *Mater. Des.*, **58**, 187-193.

Kabay, N. (2014), "Abrasion resistance and fracture energy of concretes with basalt fiber", *Constr. Build. Mater.*, **50**, 95-101.

Kizilkanat, A.B., Kabay, N., Akyüncü, V., Chowdhury, S. and Akça, A.H. (2015), "Mechanical properties and fracture behavior of basalt and glass fiber reinforced concrete: An experimental study", *Constr. Build. Mater.*, **100**, 218-224.

Lee, S.O., Rhee, K.Y. and Park, S.J. (2015), "Influence of chemical surface treatment of basalt fibers on interlaminar shear strength and fracture toughness of epoxy-based composites", *J. Ind. Eng. Chem.*, **32**, 153-156.

Li, H., Wang, W. and Zhou, W. (2014), "Fatigue damage monitoring and evolution for basalt fiber reinforced polymer materials", *Smart Struct. Syst.*, **14**(3), 307-325.

Li, W. and Xu, J. (2009), "Mechanical properties of basalt fiber reinforced geopolymeric concrete under impact loading", *Mater. Sci. Eng.: A.*, **505**(1-2), 178-186.

Murthy, A.R., Iyer, N.R. and Prasad, B.K.R. (2013), "Evaluation of mechanical properties for high strength and ultrahigh strength concretes", *Adv. Concrete Constr.*, **1**(4), 341-358.
Patel, P.A., Desai Atul, K. and Desai Jatil, A. (2012), "Evaluation of engineering properties for polypropylene fibre reinforced concrete", *Int. J. Adv. Eng. Tech.*, **3**(1), 42-45.
Pehlivanlı, Z.O., Uzun, İ. and Demir, İ. (2015), "Mechanical and microstructural features of autoclaved aerated concrete reinforced with autoclaved polypropylene, carbon, basalt and glass fiber", *Constr. Build. Mater.*, **96**, 428-433.
Peterson, P.E. (1980), "Fracture energy of concrete: Method of determination", *Cement Concrete Res.*, **10**(1), 79-89.
Shah, S.P., Swartz, S.E. and Ouyang, C. (1995), *Fracture mechanics of concrete: applications of fracture mechanics to concrete, rock and other quasi-brittle materials*, John Wiley & Sons.
Shaikh, F.U.A. (2013), "Review of mechanical properties of short fibre reinforced geopolymer composites", *Constr. Build. Mater.*, **43**, 37-49.
Sim, J., Park, C. and Moon, D.Y. (2005), "Characteristics of basalt fiber as a strengthening material for concrete structures", *Compos.*: *Part B, Eng.*, **36**(6-7), 504-512.
Sümer, Y. and Aktaş, M. (2011), "Bond length effect of fiber reinforced polymers bonded reinforced concrete beams", *Int. J. Phys. Sci.*, **6**(24), 5795-5803.
Sümer, Y. and Aktaş, M. (2014), "Finite element modeling of existing cracks on pre-loaded reinforced concrete beams", *Arab. J. Sci. Eng.*, **39**(4), 2611-2619.
Şahin, Y. and Köksal, F. (2011), "The influences of matrix and steel fibre tensile strengths on the fracture energy of high-strength concrete", *Constr. Build. Mater.*, **25**(4), 1801-1806.
Tassew, S.T. and Lubell, A.S. (2014), "Mechanical properties of glass fiber reinforced ceramic concrete", *Constr. Build. Mater.*, **51**, 215-224.

CC